1-31-2017

Working Paper No. 17017

An 8-Zone ISO-NE Test System with Physically-Based Wind Power

Wanning Li
Iowa State University, wanningl@iastate.edu

Leigh Tesfatsion
Iowa State University, tesfatsi@iastate.edu

An 8-Zone ISO-NE Test System with Physically-Based Wind Power

Wanning Li, *Student Member, IEEE,* and Leigh Tesfatsion, *Member, IEEE*

***Abstract*—This study extends the agent-based 8-Zone ISO-NE Test System to include wind turbine agents, each characterized by location, physical type, and an output curve mapping local wind speed into wind power output. Increases in wind power penetration (WPP) are modeled as build-outs of investment queues for planned wind turbine installations. The extended system is used to study the effects of increasing WPP under both stochastic and deterministic day-ahead market (DAM) formulations for security-constrained unit commitment (SCUC). For each tested WPP, the expected cost saving resulting from a switch from deterministic to stochastic DAM SCUC is found to display a U-shaped variation as the reserve requirement (RR) for deterministic DAM SCUC is successively increased. Moreover, the RR level resulting in the lowest expected cost saving systematically increases with increases in WPP.**

***Index Terms*—Wind power penetration, electric power system, agent-based test system, wind turbine agents, day-ahead market, security-constrained unit commitment, stochastic optimization**

NOMENCLATURE FOR SCUC FORMULATIONS

***Sets*:**

$\mathbb{G}$	Set of all dispatchable generators g
$\mathbb{G}(z)$	Set of dispatchable generators g at zone z
$\mathbb{L} \subset \mathbb{Z} \times \mathbb{Z}$	Set of transmission lines ℓ
$\mathbb{L}_O(z)$	Subset of lines ℓ originating at zone z
$\mathbb{L}_E(z)$	Subset of lines ℓ ending at zone z
$\mathbb{S}$	Set of scenarios s
$\mathbb{T}$	Set of hourly time periods $t = 1, \ldots, T$
$\mathbb{Z}$	Set of zones z

***Input Parameters*:**

a_g	Production cost coefficient (\$/MW) for g
b_g	Production cost coefficient (\$/(MW)^2) for g
B_ℓ	Inverse of reactance (pu) on line ℓ
$c_{cold,g}$	Cold-start cost coefficient (\$) for g
$c_{hot,g}$	Hot-start cost coefficient (\$) for g required to satisfy $c_{hot,g} \leq c_{cold,g}$
$c_{D,g}$	Shut-down cost coefficient (\$) for g
$c_{N,g}$	No-load cost coefficient (\$) for g
$E(\ell)$	End zone for line ℓ
f_ℓ^{max}	Power limit for transmission line ℓ
$NL_z^s(t)$	Zone-z net load in hour t, given s
$L_z^s(t)$	Zone-z load in hour t, given s
$O(\ell)$	Originating zone for line ℓ
P_g^{max}	Maximum power limit for g
P_g^{min}	Minimum power limit for g
RR	System-wide spinning reserve requirement (MW) for deterministic DAM SCUC
$R_{D,g}$	Online ramp-down rate (MW/Δt) for g
$RT_{D,g}$	$\min\{P_g^{max}, R_{D,g}\Delta t\}$ (MW) for each g
$R_{U,g}$	Online ramp-up rate (MW/Δt) for g
$RT_{U,g}$	$\min\{P_g^{max}, \cdot R_{U,g}\Delta t\}$ (MW) for each g
$R_{SD,g}$	Shut-down ramp rate (MW/Δt) for g
$RT_{SD,g}$	$\min\{P_g^{max}, R_{SD,g}\Delta t\}$ (MW) for each g
$R_{SU,g}$	Start-up ramp rate (MW/Δt) for g
$RT_{SU,g}$	$\min\{P_g^{max}, R_{SU,g}\Delta t\}$ (MW) for each g
S_o	Positive base power (in three-phase MVA)
$T_{cold,g}$	No. of cold-start hours for g[1]
$T_{D,g}$	Minimum down-time for g (in hours)
$T_{U,g}$	Minimum up-time for g (in hours)
$T_{\text{off},g}$	No. of hours that g must be initially offline if $0 > \hat{v}_g(0)$; 0 if $0 < \hat{v}_g(0)$
$T_{\text{on},g}$	No. of hours that g must be initially online if $0 < \hat{v}_g(0)$; 0 if $0 > \hat{v}_g(0)$
$\hat{v}_g(0)$	g's on/off status in hour 0[2]
$W_z^s(t)$	Zone-z wind power in hour t, given s
$\alpha_z^s(t)$	Power-balance slack term (MW) at zone z in hour t, given s
Δt	Time-period length (one hour)
$\gamma_z^s(t)$	Absolute value of $\alpha_z^s(t)$
Γ	Penalty (\$/MW) for power-balance slack
π^s	Probability of scenario s

***Variables and Functions*:**

ISO Decision Variables:

$p_g^s(t)$	Power output for g in hour t, given s
$v_g(t)$	g's on/off status (1/0) in hour t
$\theta_z^s(t)$	Voltage angle (radians) at zone z in hour t, given s

Functions of ISO Decision Variables:

$C_{D,g}(t)$	Shut-down cost (\$) for g in hour t
$C_{N,g}(t)$	No-load cost (\$) for g in hour t
$C_{U,g}(t)$	Start-up cost (\$) for g in hour t
$C_{P,g}^s(t)$	Dispatch cost (\$) for g in hour t, given s
$f_\ell^s(t)$	Power on line ℓ in hour t, given s
$H_g(t)$	Hot-start indicator for g; a value of 1 (0) indicates a hot (cold) start for g in hour t
$\overline{p}_g^s(t)$	Maximum available power output for g in hour t, given s

Latest revision: 1 Feb 2017. W. Li (wanningli.ee@gmail.com) is with the Department of Electrical and Computer Engineering, and L. Tesfatsion (tesfatsi@iastate.edu) is with the Department of Economics, both at Iowa State University, Ames, IA 50011 USA. This work has been supported in part by DOE awards DE-AR00002014 and DE-OE0000839.

[1] If generator g at the start of hour t has been off-line for at least $T_{\text{cold},g}$ consecutive hours prior to t, any start-up of g in t incurs the cold-start cost $c_{\text{cold},g}$. Otherwise, any start-up of g in hour t incurs the hot-start cost $c_{\text{hot},g}$.

[2] A positive (negative) value for $\hat{v}_g(0)$ indicates the number of hours prior to and including hour 0 that generator g has been turned on (off). Note that the value of $\hat{v}_g(0)$ cannot be zero.

I. Introduction

WIND is one of the fastest-growing sources of electric power in the U.S. and has been the largest new source of renewable energy for the U.S. during the past decade [1]. The U.S. is on track for achieving the wind energy goal set out in the Wind Vision Report [2]: namely, 35% of the nation's end-use electricity demands met by wind power by 2050.

Numerous researchers have sought to estimate the potential impacts of growing *wind power penetration (WPP)* on existing power system operations (e.g., [3], [4], [5], [6]). Other researchers have proposed changes in existing power system operations to better handle the increased uncertainty associated with increased WPP [7]. For example, new forms of stochastic and robust optimization are explored in ([8],[9]), while improved methods for the dynamic specification of *reserve requirement (RR)* levels are proposed in [10], [11], and [12, Parts I-II].

In these studies, WPP increases are typically modeled as scaled-up versions of historically observed wind power levels. However, this simple method cannot account for differences in wind power generation arising from the combined effects of local weather conditions, changes in the mix of wind turbine types, and changes in the geographical placement of wind turbines. Thus, how to model WPP increases in a practical empirically-realistic way remains an open challenge.

This study uses a novel agent-based method to extend a previously developed agent-based 8-Zone ISO-NE Test System [13] by inclusion of physically-based wind turbine agents. This permits WPP increases to be modeled in a manner reflecting the way actual WPP increases take place over time in an energy region such as ISO-NE: namely, through additional wind turbine investments. To illustrate the method in concrete terms, the extended test system is used to compare the performance of stochastic versus deterministic formulations for *security-constrained unit commitment (SCUC)* in a *day-ahead market (DAM)* under systematically varied WPP and RR levels.

The remainder of this paper is organized as follows. Section II reviews the core features of the AMES Wholesale Power Market Test Bed, and Section III describes the Eight-Zone ISO-NE Test System, based on AMES(V4.0), which is the foundation for all sensitivity testing reported in this study.

Our agent-based method for the construction of wind power scenarios and WPP increases is explained in Section IV. Section V presents two alternative DAM SCUC formulations, stochastic and deterministic. Section VI presents our sensitivity design for testing the performance of these DAM SCUC formulations under systematically varied values for two key treatment factors: the WPP level; and the RR level for deterministic SCUC. Key findings are presented and discussed in Section VII. Section VIII concludes.

II. The AMES Test Bed

The AMES (*A*gent-based *M*odeling of *E*lectricity *S*ystems) Test Bed [14] is an agent-based computational laboratory permitting the dynamic study of wholesale power markets operating over AC transmission grids subject to congestion. AMES incorporates, in simplified form, the core features of the two-settlement system design proposed by the Federal Energy Regulatory Commission for U.S. wholesale power markets [15]. To date, this design has been adopted in seven U.S. energy regions (CAISO, ERCOT, ISO-NE, MISO, NYISO, PJM, SPP) encompassing over 60% of U.S. generation capacity.

The version of AMES used in the present study (V4.0) is a modular extensible platform developed primarily in Java, with calls to an external Python routine for handling successive daily SCUC optimizations. As depicted in Fig. 1, and carefully discussed in [13, Section II], the key features of AMES(V4.0) are as follows:

1) **Market Participants:** These include *Load Serving Entities (LSEs)* that demand electric power in order to service the loads of their retail customers as well as *Generation Companies (GenCos)* that produce and supply electric power from both dispatchable and non-dispatchable resources. Each participant is modeled as a private business entity whose goal is to secure the highest possible net earnings from its market activities over time. At the beginning of each simulation run, the user-specified methods of the LSEs and dispatchable GenCos include demand bid and supply offer functions, and they can also include learning algorithms permitting the endogenous updating of these functions over time.
2) **Central Management:** Market and system operations are centrally managed by a non-profit *Independent System Operator (ISO)* whose goal is to maintain the reliable and efficient operation of the wholesale power system over time.
3) **Two-Settlement System:** On each successive day the ISO conducts a bid/offer-based *Day-Ahead Market (DAM)* to determine hourly resource commitments and dispatch levels for next-day operations as well as a *Real-Time Market (RTM)* to correct for any imbalances between day-ahead dispatch schedules and real-time power needs. Each market is separately settled by *Locational Marginal Pricing (LMP),* i.e., the pricing of power by the timing and location of its withdrawal from, or injection into, the transmission grid.
4) **AC Transmission Grid.** The LSEs and GenCos are located at user-specified locations across the AC transmission grid. Congestion is managed via LMP.

III. The Eight-Zone ISO-NE Test System

The ISO New England (ISO-NE) is an independent non-profit Regional Transmission Organization (RTO) serving the following six New England states: Connecticut, Maine, Massachusetts, New Hampshire, Rhode Island, and Vermont. The agent-based 8-Zone ISO-NE Test System, originally developed in [13], is a specialization of AMES(V4.0) based on structural attributes and data from the ISO-NE that has been successfully used for test case development in ([16], [17], [18], [19]).

Specifically, in accordance with actual ISO-NE practice [20], the 8-Zone ISO-NE Test System divides the ISO-NE energy region into eight load zones: namely, Connecticut (CT), Maine (ME), New Hampshire (NH), Rhode Island (RI), Vermont (VT), Northeastern Massachusetts/Boston

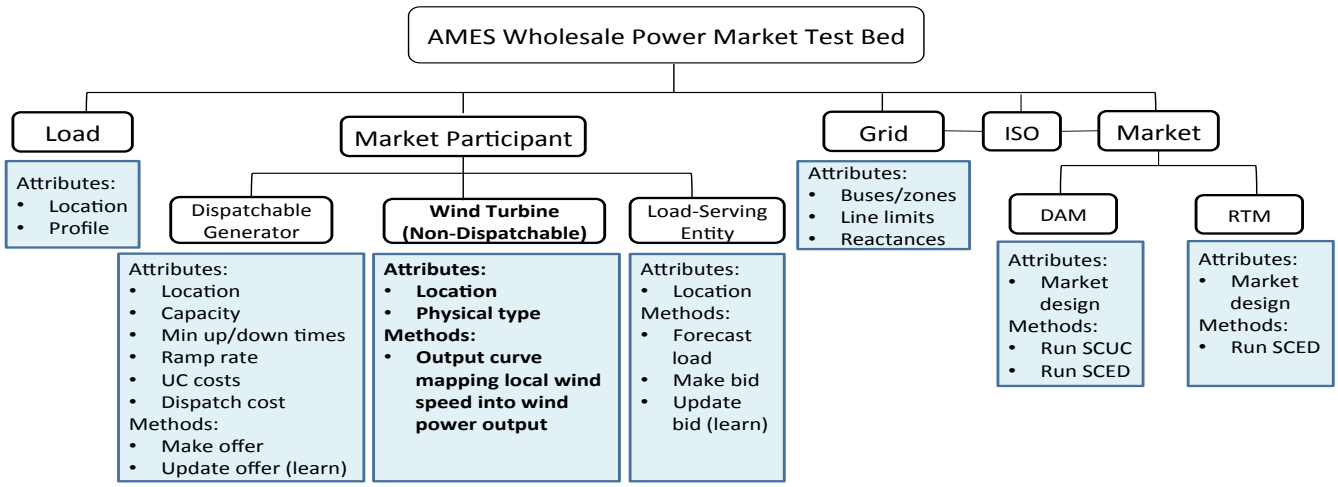

Fig. 1. Key features of AMES(V4.0) extended to include wind turbine agents

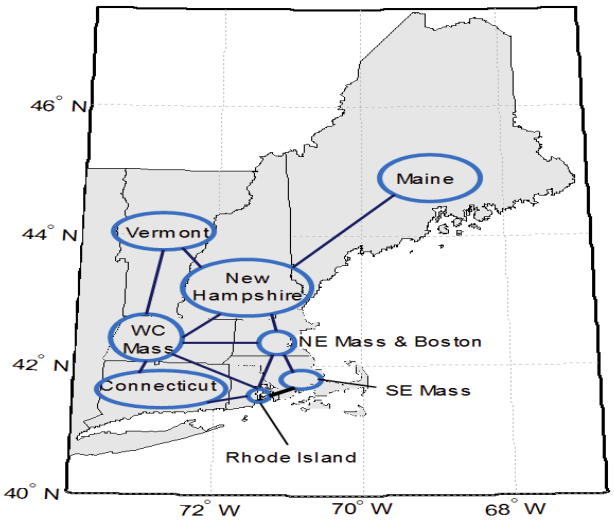

Fig. 2. Transmission grid for the 8-Zone ISO-NE Test System

(NEMA/BOST), Southeastern Massachusetts (SEMA), and Western/Central Massachusetts (WCMA). As shown in Fig. 2, the AC transmission grid connecting these eight load zones is approximated by a meshed network consisting of twelve transmission lines whose length, resistance, and reactance attributes are calibrated on the basis of ISO-NE data.

As detailed in [13, Section III.B], the mix of 76 thermal generators for the 8-Zone ISO-NE Test System is a scaled-down version of the actual ISO-NE thermal mix in 2015. The fuel types of these 76 thermal generators include natural gas (47%), fuel oil (23%), nuclear (20%), and coal (10%), with a total capacity of about 23GW. Start-up costs, no-load costs, minimum up/down time constraints, ramping constraints, and quadratic production cost function approximations for each of the 76 thermal generators are based on ISO-NE and EIA data.

Complete code and benchmark data configuration files for the 8-Zone ISO-NE Test System can be obtained at a code/data repository site [21].

IV. Agent-Based Modeling of Wind Penetration

A. Overview of approach

This study extends the agent-based 8-Zone ISO-NE Test System [13] to include wind turbine agents. As depicted in Fig. 1, a wind turbine agent is characterized at each point in time by its attributes and methods. Its attributes include its location (zone) and its physical aspects as determined by its turbine type. Its methods include an output curve mapping local wind speed into wind power output.

The base wind power penetration level specified for our sensitivity tests is actual wind power capacity in ISO-NE in 2013, as reported in the 2013 New England Wind Integration Study (NEWIS) [22]. Possible increases in wind power penetration are modeled as build-outs of ISO-NE's wind investment queues as reported in this same study.

B. Approach details

The 2013 NEWIS [22] develops five categories of wind build-out scenarios to represent successively greater wind power penetration levels that could potentially be implemented for ISO-NE. These build-out scenarios are categorized by their aggregate installed nameplate capacity for onshore and offshore wind power and by their simulated contribution to the servicing of forecasted annual load for ISO-NE as a whole.

For the purposes of this study, *Wind Power Penetration (WPP)* in any given year is defined to be the percentage contribution of wind power to the servicing of load for that year. Formally:

$$\text{WPP} = \frac{\text{Annual Wind Power}}{\text{Annual Load}} \times 100\% \qquad (1)$$

Three distinct WPP treatments at levels 2%, 10%, and 20% are constructed from the NEWIS build-out scenarios. The 2% WPP treatment represents the actual state of wind power development in ISO-NE in 2013. The 10% and 20% WPP treatments represent potential future build-outs of wind investment queues in ISO-NE that would result in medium and high wind power penetration levels, respectively. The wind sites under each of these treatments are shown in Fig. 3.

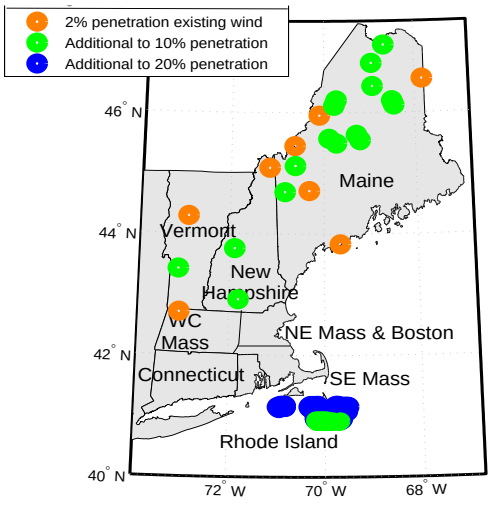

Fig. 3. Location of existing and potential wind sites for ISO-NE corresponding to 2%, 10% and 20% wind power penetration levels. Source: [22]

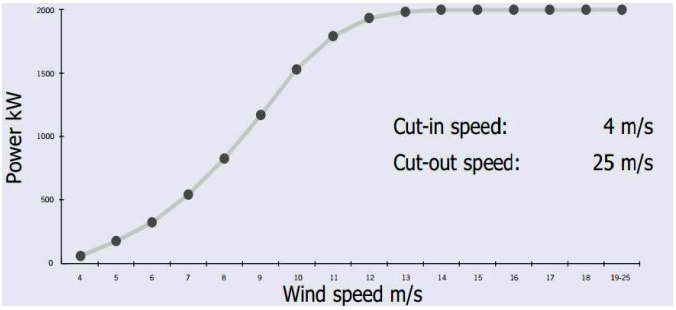

Fig. 4. Output curve mapping wind speed into wind power output for the Gamesa G87 (2MW) wind turbine. Source: [23]

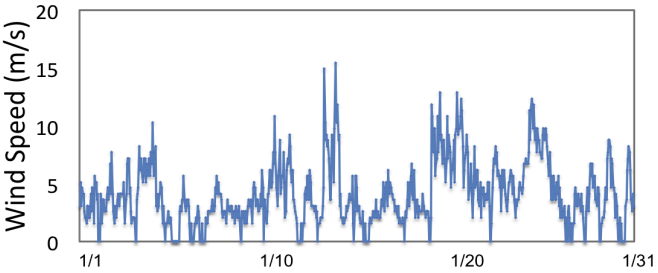

Fig. 5. Wind speed at Hartford, Connecticut, from 1/1/2016 to 1/31/2016. Source: [24]

The benefit of using data from the 2013 NEWIS [22] to construct WPP treatments is that nameplate capacities of onshore and offshore wind, as well as loads, are reported for individual ISO-NE states as well for the ISO-NE as a whole. This permits us to map this information into the eight load zones comprising the 8-Zone ISO-NE Test System; cf. Fig. 2. However, this information is not sufficient to determine wind power outputs at the level of individual wind turbines.

To address this gap, the following four steps were taken for each WPP treatment (2%, 10%, and 20%). First, we roughly specified the number and types of wind turbines to be located within each of the eight test system load zones using the NEWIS build-out scenario corresponding to the given WPP treatment. Second, we obtained time-series data for wind speed within each zone. Third, for each type of wind turbine in each zone, we specified an appropriate output curve mapping local wind speed into wind power output. Fourth, making use of local wind speed data, turbine physical characteristics, and turbine output curves, we refined the number and types of wind turbines located within each zone to be consistent with the given WPP treatment.[3]

The output curves corresponding to different types of wind turbines were specified as in [23]. For example, the output curve for the Gamesa G87 (2MW) type of wind turbine installed in Massachusetts (MA) is depicted in Fig. 4.

Real-world wind speed data were obtained by location and time for ISO-NE from the Iowa Environmental Mesonet (IEM) ([24], [25]). The IEM collects environmental data from cooperating members and maintains automated airport weather observations from around the world. For instance, the Connecticut weather data accessible at [24] includes wind speed, wind direction, temperature, humidity and altimeter readings. Figure 5 depicts the wind speed profile from 1/1/2016 to 1/31/2016 for Hartford, Connecticut.

[3]For each WPP treatment, 2013 ISO-NE aggregate load was used for the denominator of the WPP measure (1). For this study we did not attempt to forecast investment-queue build-out times and load changes over these times.

V. Two Alternative DAM SCUC Formulations

A. SCUC Formulation Overview

The stochastic DAM SCUC formulation used in this study is a stochastic version of the well-known SCUC formulation developed in [26]. The deterministic DAM SCUC formulation used in this study is derived from the stochastic DAM SCUC formulation by replacing net load scenarios with expected net load and by including a system-wide reserve requirement.

B. Stochastic DAM SCUC Formulation

The objective of the stochastic DAM SCUC formulation is to minimize expected total energy cost subject to standard unit commitment and system constraints. Expectations are taken with respect to a set $\mathbb{S}$ of possible scenarios for future *net load*, i.e., load minus wind power.[4] Wind power is treated as negative load since it is assumed to be non-dispatchable generation with zero operating costs.

Expected total energy cost is the summation of *first-stage costs* (i.e., DAM UC costs) plus the expected level of *second-stage costs* (i.e., real-time dispatch costs plus penalty costs imposed for real-time wind spillage or load curtailment).

The ISO decision variables are correspondingly classified as follows:

- First-stage decision variables: Generator on/off commitment indicator variables, not scenario-conditioned

[4]The construction of $\mathbb{S}$ is detailed in Section VI-A.

- Second-stage decision variables: Scenario-conditioned generator dispatch and voltage angle levels

Objective function to be minimized:

$$\sum_{t\in\mathbb{T}}\sum_{g\in\mathbb{G}}[C_{U,g}(t)+C_{N,g}(t)+C_{D,g}(t)] + \sum_{s\in\mathbb{S}}\pi^s\sum_{t\in\mathbb{T}}\sum_{g\in\mathbb{G}}C^s_{P,g}(t)+\Gamma\sum_{s\in\mathbb{S}}\pi^s\sum_{z\in\mathbb{Z}}\sum_{t\in\mathbb{T}}\gamma^s_z(t) \quad (2)$$

ISO decision variables:

$$v_g(t),\ p^s_g(t),\ \theta^s_z(t),\quad \forall s\in\mathbb{S}, z\in\mathbb{Z}, t\in\mathbb{T}, g\in\mathbb{G} \quad (3)$$

ISO decision variable bounds:

$$v_g(t)\in\{0,1\} \qquad \forall t\in\mathbb{T}, g\in\mathbb{G} \quad (4)$$

$$0\le p^s_g(t)\le P^{max}_g \qquad \forall s\in\mathbb{S}, t\in\mathbb{T}, g\in\mathbb{G} \quad (5)$$

$$-\pi\le\theta^s_z(t)\le\pi \qquad \forall s\in\mathbb{S}, z\in\mathbb{Z}, t\in\mathbb{T} \quad (6)$$

Start-up cost constraints $\forall g\in\mathbb{G}$:

$$C_{U,g}(t)=\max\{0,U_g(t)\};$$
$$U_g(t)=c_{cold,g}-[c_{cold,g}-c_{hot,g}]H_g(t) - c_{cold,g}\big[1-[v_g(t)-v_g(t-1)]\big],\ \forall t\in\mathbb{T} \quad (7)$$

Hot start-up constraints $\forall g\in\mathbb{G}$:

$$H_g(t)=1 \text{ if: } 1\le t\le T_{cold,g};\ (t-T_{cold,g})\le\hat{v}_g(0) \quad (8)$$

$$H_g(t)\le\sum_{\tau=1}^{t-1}v_g(\tau) \text{ if: } 1\le t\le T_{cold,g};\ (t-T_{cold,g})>\hat{v}_g(0) \quad (9)$$

$$H_g(t)\le\sum_{\tau=t-T_{cold,g}}^{t-1}v_g(\tau) \text{ if: } (T_{cold,g}+1)\le t\le T \quad (10)$$

No-load cost constraints $\forall g\in\mathbb{G}$:

$$C_{N,g}(t)=c_{N,g}v_g(t) \qquad \forall t\in T \quad (11)$$

Shut-down cost constraints $\forall g\in\mathbb{G}$:

$$C_{D,g}(t)=\max\{0,D_g(t)\};$$
$$D_g(t)=c_{D,g}[v_g(t-1)-v_g(t)], \qquad \forall t\in\mathbb{T} \quad (12)$$

Production costs $\forall g\in\mathbb{G}$ (scenario-conditioned):

$$C^s_{P,g}(t)=a_gp^s_g(t)+b_g[p^s_g(t)]^2,\ \forall s\in\mathbb{S}, t\in\mathbb{T} \quad (13)$$

Power balance constraints $\forall z\in\mathbb{Z}$ (scenario-conditioned):

$$\sum_{g\in\mathbb{G}(z)}p^s_g(t)+\sum_{\ell\in\mathbb{L}_E(z)}f^s_\ell(t)+\alpha^s_z(t) = NL^s_z(t)+\sum_{\ell\in\mathbb{L}_O(z)}f^s_\ell(t);$$
$$\alpha^s_z(t)=\alpha^{+,s}_z(t)-\alpha^{-,s}_z(t);$$
$$\gamma^s_z(t)=\alpha^{+,s}_z(t)+\alpha^{-,s}_z(t);$$
$$\forall s\in\mathbb{S}, t\in\mathbb{T} \quad (14)$$

Line limit constraints $\forall\ell\in\mathbb{L}$ (scenario-conditioned):

$$f^s_\ell(t)=S_oB_\ell\left[\theta^s_{O(\ell}(t)-\theta^s_{E(\ell)}(t)\right], \quad (15)$$

$$-f^{max}_\ell\le f^s_\ell(t)\le f^{max}_\ell, \qquad \forall s\in\mathbb{S}, t\in\mathbb{T} \quad (16)$$

Capacity constraints $\forall g\in\mathbb{G}$ (scenario-conditioned):

$$P^{min}_gv_g(t)\le p^s_g(t)\le\bar{p}^s_g(t)\le P^{max}_gv_g(t) \qquad \forall s\in\mathbb{S}, t\in\mathbb{T} \quad (17)$$

Ramp constraints $\forall g\in\mathbb{G}$ (scenario-conditioned):

$$\bar{p}^s_g(t)-p^s_g(t-1)\le RT_{U,g}v_g(t-1) + RT_{SU,g}[v_g(t)-v_g(t-1)] + P^{max}_g[1-v_g(t)], \quad \forall s\in\mathbb{S}, t\in\mathbb{T}; \quad (18)$$

$$\bar{p}^s_g(t)-P^{max}_gv_g(t+1)\le RT_{SD,g}[v_g(t)-v_g(t+1)], \quad \forall s\in\mathbb{S},\ 1\le t\le T-1; \quad (19)$$

$$p^s_g(t-1)-p^s_g(t)\le RT_{D,g}v_g(t) + RT_{SD,g}[v_g(t-1)-v_g(t)] + P^{max}_g[1-v_g(t-1)], \quad \forall s\in\mathbb{S}, t\in\mathbb{T} \quad (20)$$

Minimum up-time constraints $\forall g\in\mathbb{G}$:

$$\sum_{\tau=1}^{T_{\text{on},g}}[1-v_g(\tau)]=0 \text{ if } T_{\text{on},g}\ge1; \quad (21)$$

$$\sum_{\tau=t}^{t+T_{U,g}-1}v_g(\tau)\ge T_{U,g}[v_g(t)-v_g(t-1)] \text{ for } (T_{\text{on},g}+1)\le t\le(T-T_{U,g}+1); \quad (22)$$

$$\sum_{\tau=t}^{T}\big(v_g(\tau)-[v_g(t)-v_g(t-1)]\big)\ge0 \text{ for } (T-T_{U,g}+1)<t\le T \quad (23)$$

Minimum down-time constraints $\forall g\in\mathbb{G}$:

$$\sum_{\tau=1}^{T_{\text{off},g}}v_g(\tau)=0 \text{ if } T_{\text{off},g}\ge1; \quad (24)$$

$$\sum_{\tau=t}^{t+T_{D,g}-1}[1-v_g(\tau)]\ge T_{D,g}[v_g(t-1)-v_g(t)] \text{ for } (T_{\text{off},g}+1)\le t\le(T-T_{D,g}+1); \quad (25)$$

$$\sum_{\tau=t}^{T}\big([1-v_g(\tau)]-[v_g(t-1)-v_g(t)]\big)\ge0 \text{ for } (T-T_{D,g}+1)<t\le T \quad (26)$$

Voltage angle constraints for angle reference zone 1:

$$\theta^s_1(t)=0, \quad \forall s\in\mathbb{S}, t\in\mathbb{T} \quad (27)$$

C. Deterministic DAM SCUC Formulation with Reserve

The deterministic DAM SCUC formulation used in this study is derived from the stochastic DAM SCUC formulation presented in Section V-B in two steps.

First, the scenario set $\mathbb{S}$ for the stochastic formulation is everywhere replaced in the objective function and system constraints by a single net load scenario $\bar{s}$ calculated as the expectation (probability-weighted average) of the net load scenarios s in $\mathbb{S}$. Thus, for example, the objective function for

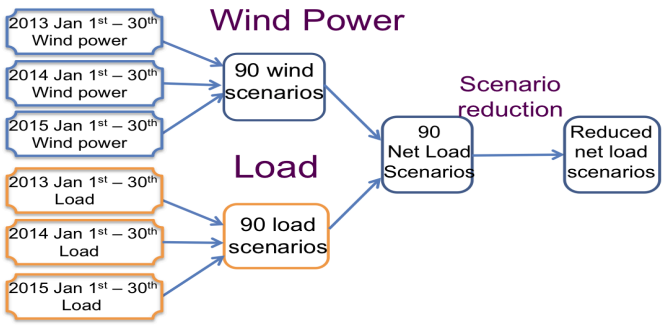

Fig. 6. Construction of the net load scenario set $\mathbb{S}^{wpp}$ for each given WPP

the deterministic DAM SCUC formulation takes the following reduced form:

$$\sum_{t\in\mathbb{T}}\sum_{g\in\mathbb{G}}\left[C_{U,g}(t)+C_{N,g}(t)+C_{D,g}(t)+C^{\bar{s}}_{P,g}(t)\right] + \Gamma\sum_{z\in\mathbb{Z}}\sum_{t\in\mathbb{T}}\gamma^{\bar{s}}_{z}(t) \quad (28)$$

Second, the resulting reduced-form constraints are augmented to include the following system-wide spinning reserve requirement constraints: For each hour $t \in \mathbb{T}$,

$$\sum_{g\in\mathbb{G}}\overline{p}^{\bar{s}}_{g}(t) \geq \sum_{z\in\mathbb{Z}} NL^{\bar{s}}_{z}(t) + RR \quad (29)$$

The determination of the spinning reserve requirement RR in (29) is explained below in Section VI-B.

VI. Sensitivity Design

A. Construction of WPP-Dependent Net Load Scenario Sets

As detailed in Section IV-B, each WPP treatment considered in this study is associated with a distinct mix of wind turbines distributed across the eight zones of the 8-Zone ISO-NE Test System; cf. Fig. 3. Consequently, for each WPP treatment, a given pattern of loads and wind speeds across these eight zones results in a distinct WPP-dependent pattern of wind power outputs and hence a distinct WPP-dependent pattern of net loads, defined to be load minus wind power.

For each WPP treatment, a set $\mathbb{S}^{wpp}$ of two-day (48 hour) net load scenarios was constructed, making use of: (i) historical load and wind speed data for the ISO-NE; and (ii) the relevant wind turbine output curves for this particular WPP treatment. Each scenario $s \in \mathbb{S}^{wpp}$ takes the form

$$s \;=\; \big(s(z1),\ldots,s(z8)\big) \quad (30)$$

where, for each $i = 1,\ldots,8$,

$$s(zi) = \big(NL^{s}_{zi}(1), NL^{s}_{zi}(2),\ldots,NL^{s}_{zi}(48)\big) \quad (31)$$

and

$$NL^{s}_{zi}(t) = L^{s}_{zi}(t) - W^{s}_{zi}(t)\,,\; t = 1,\ldots,48 \quad (32)$$

More precisely, as depicted in Fig. 6, the construction of each $s \in \mathbb{S}^{wpp}$ proceeded as follows. We first constructed 90 two-day (48 hour) load scenarios and 90 two-day (48 hour) wind power scenarios for each zone $zi, i = 1,\ldots,8$. This construction made use of (i) ISO-NE zonal load and wind speed data ([24], [27]) for the month of January for three successive years 2013-2015, and (ii) WPP-conditional wind turbine output curves [23] allowing us to map wind speeds to wind power outputs for the wind turbines in each zone.

Second, we derived 90 net load scenarios $\hat{s} = (s(z1),\ldots,s(z8))$ from these 90 load and wind power scenarios by subtracting wind power from load for each zone for each successive hour. Third, we assigned a probability of 1/90 to each net load scenario $\hat{s}$. Fourth, we applied a well-known scenario reduction method ([28], [29]) based on similarity clustering to reduce this set of 90 net load scenarios $\hat{s}$ to a smaller set $\mathbb{S}^{wpp}$ containing only ten net load scenarios s. Fifth, each s in $\mathbb{S}^{wpp}$ was assigned a probability π^{s} equal to the sum of the probabilities for the original net load scenarios lying in its cluster.

For each WPP treatment, the elements $s \in \mathbb{S}^{wpp}$ are assumed to be the net load scenarios that the ISO anticipates could be realized for zones $z1,\ldots,z8$ over days D and D+1 from the vantage point of the DAM on the current day D-1.

B. Treatment Factors

Two treatment factors are considered in this study: (i) wind power penetration (WPP) as defined by (1); and (ii) the reserve requirement (RR) for deterministic SCUC appearing in (29). As detailed in Section IV-B, the three tested WPP treatments are 2%, 10%, and 20%. For each WPP treatment, the same eleven RR treatments are tested: namely, 0MW, 500MW, 1000MW, …, 5000MW. These eleven RR values were selected so that, for each WPP treatment, reserve expressed as a percentage of peak net load ranges from 0% to 30%.[5]

C. Performance Metric

The metric used to compare the performance of the stochastic and deterministic DAM SCUC formulations is expected cost saving, calculated as the percentage difference in expected total energy cost when the ISO switches from a deterministic to a stochastic DAM SCUC formulation. As detailed in Section V-B, total energy cost includes start-up, no-load, shut-down, dispatch, and penalty costs.

As depicted in Fig. 7, no-load, start-up, and shut-down costs are "first stage" UC costs determined in the DAM SCUC optimization. Dispatch costs and penalty costs for wind spillage or load curtailment are "second stage" costs determined by *security-constrained economic dispatch (SCED)* in the *real-time market (RTM)* on the basis of actual real-time net load.[6]

For each (WPP,RR) treatment, the (second-day) expected cost saving is calculated as follows.

1) Select a net load scenario sj from the ten net load scenarios in $\mathbb{S}^{wpp}$ to be the simulated-true net load scenario for the next two days.

[5]For each WPP, peak net load PNL^{wpp} is defined to be the highest possible hourly aggregate net load that could be realized given the ten possible net load scenarios in $\mathbb{S}^{wpp}$. For each (WPP,RR), reserve expressed as a percentage of peak net load is then given by $RRP^{wpp} = RR/PNL^{wpp}$.

[6]For simplicity, it is assumed in this study that ISO-forecasted net load in the RTM coincides with actual real-time net load.

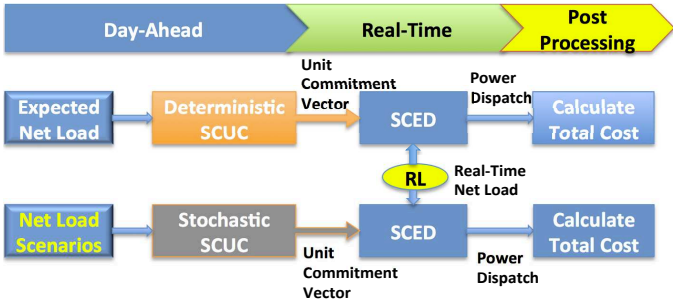

Fig. 7. Comparative performance testing procedure for the stochastic vs. deterministic DAM SCUC formulations

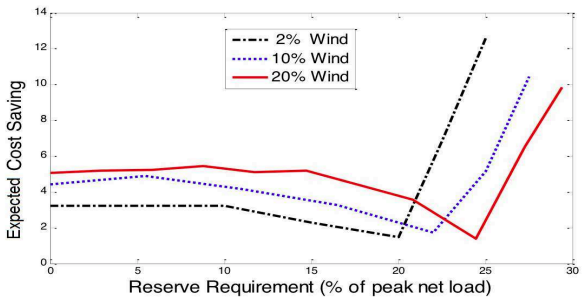

Fig. 8. Expected cost saving as a function of the reserve requirement RR for deterministic DAM SCUC, conditional on wind power penetration (WPP)

2) Calculate the total energy cost over each of the next two days, given WPP, RR, and sj, when the ISO uses deterministic DAM SCUC augmented with an RR constraint, conditional on the expected net load scenario $\bar{s}$ constructed from $\mathbb{S}^{wpp}$ and its associated probabilities π^s, $s \in \mathbb{S}^{wpp}$.
3) Calculate the total energy cost over each of the next two days, given WPP and sj, when the ISO uses stochastic DAM SCUC conditional on $\mathbb{S}^{wpp}$ and its associated probabilities π^s, $s \in \mathbb{S}^{wpp}$.
4) Let $\text{TC}^{wpp}_{rr,sj}(\text{Det})$ and $\text{TC}^{wpp}_{sj}(\text{Sto})$ denote the total energy cost resulting on the *second* day from deterministic and stochastic DAM SCUC, respectively. Calculate the (second-day) *Cost Saving* that would result from a switch from a deterministic to a stochastic DAM SCUC, given WPP, RR, and sj, as follows:

$$\text{CS}^{wpp}_{rr,sj} = \frac{\text{TC}^{wpp}_{rr,sj}(\text{Det}) - \text{TC}^{wpp}_{sj}(\text{Sto})}{\text{TC}^{wpp}_{rr,sj}(\text{Det})} \times 100\% \qquad (33)$$

5) Repeat steps 1) through 4) for each of the ten load scenarios $s1, \ldots, s10$ in $\mathbb{S}^{wpp}$, and calculate the (second-day) *expected cost saving*, given WPP and RR, as

$$\text{Exp}[\text{CS}^{wpp}_{rr}] = \sum_{j=1}^{10} \pi^{sj} \text{CS}^{wpp}_{rr,sj} \qquad (34)$$

D. Software Implementation

All simulations were implemented by running the AMES(V4.0) test bed [14] on an Intel(R) Core(TM) 2 Duo CPU E8400 @ 3Ghz machine. AMES(V4.0) uses 64-bit versions of Java (v1.8.0_25), Coopr (v3.4.7842), Python (v2.7.8), MatLab(v2014a) and CPLEX Studio (v12.51). Two threads were used to solve the DAM SCUC optimizations.

VII. Key Findings for Sensitivity Study

Figure 8 reports expected cost saving (34) as a function of the reserve requirement (RR), conditional on three distinct wind power penetration (WPP) settings: low (2%), moderate (10%), and high (20%). For clarity of exposition, RR settings are expressed as percentages of peak net load; cf. footnote 5.

One key regularity seen in Fig. 8 is the generic U-shape of expected cost saving as a function of RR. For each given WPP treatment, expected cost saving initially remains relatively flat as RR is increased and then begins to decline. As RR continues to increase, RR reaches a "sweet spot" where expected cost saving is minimized, i.e., where deterministic SCUC does best in comparison to stochastic SCUC in terms of expected total energy cost. As RR continues to increase, however, expected cost saving dramatically rises.

The intuitive explanation for this generic U-shape is as follows. No matter which net load scenario is realized in real time, stochastic DAM SCUC must ensure real-time balancing of this net load by an appropriate commitment of generation. On the other hand, deterministic DAM SCUC commits only enough generation to balance *expected* real-time net load plus meet its reserve requirement.

Given a sufficiently low RR, deterministic DAM SCUC commits less generation than stochastic DAM SCUC, resulting in lower unit commitment (UC) costs; but it also runs the risk its commitment will be insufficient to meet real-time net load. In this case, to attain balance, either resort must be made to more expensive "peaker" generation units or a penalty Γ ($/MW) must be paid for wind spillage and/or load shedding as measured by the appearance of non-zero slack terms $\alpha^s_z(t)$ in the power balance constraints (14). Conversely, given a high RR, deterministic DAM SCUC must resort to a high commitment of generation to meet its high reserve requirement; hence, its UC costs are high regardless of the expected net load.

On the other hand, the commitment for stochastic DAM SCUC does not depend on RR. Consequently, the expected cost saving resulting from a switch from deterministic to stochastic SCUC is positive for sufficiently low or high RR settings, dramatically so for very high RR settings. Moreover, even at the sweet-spot RR setting most favorable to deterministic SCUC, expected cost saving remains positive.[7]

A second regularity seen in Fig. 8 is that the sweet-spot RR setting systematically increases with increases in WPP. At higher WPP levels there is more net load *volatility*. Thus, starting from a sweet-spot RR setting for a given WPP, an increase in WPP implies that deterministic SCUC faces a greater risk its unit commitment, selected to balance *expected*

[7]Interestingly, in the comparative SCUC study conducted in [13] in the absence of non-dispatchable generation, expected cost saving also displays a U-shaped variation with respect to changes in RR. However, expected cost saving actually turns negative at the sweet-spot RR setting, meaning deterministic SCUC strictly outperforms stochastic SCUC at this setting.

real-time net load, will be insufficient to balance *actual* real-time net load and hence will result in higher total energy costs. To reduce these higher expected total energy costs, the only possible option is to increase RR. Note from (33) and (34) that any reduction in expected total energy costs for deterministic SCUC due to an increase in RR implies a decrease in expected cost saving because expected total energy costs for stochastic SCUC do not depend on RR.

VIII. Conclusion

This study develops a novel agent-based method for the modeling of wind power penetration (WPP). Increases in WPP are implemented as build-outs of wind-power investment queues, resulting in additional installations of wind turbines. Each wind turbine is characterized by location, physical type, and an output curve mapping local wind speed into wind power output. This method thus permits fixed data sets for wind speeds and loads to be used to examine the effects of increases in WPP that would arise under variously proposed plans for future wind turbine installations.

To demonstrate the practical use of this method, a previously developed agent-based 8-Zone ISO-NE Test System [13] is extended to include physically-based wind turbine agents, each characterized by location, physical type, and output curve. The resulting extended test system is used to explore the effects of increasing WPP, modeled as ISO-NE investment queue build-outs, under two alternative DAM SCUC formulations: (i) deterministic DAM SCUC conditional on an expected net load scenario and a system-wide spinning reserve requirement (RR); and (ii) stochastic DAM SCUC conditional on an ensemble of net load scenarios with associated probabilities.

One key reported finding is that the expected cost saving resulting from a switch from (i) to (ii) is a U-shaped function of RR for each tested WPP level. Moreover, as WPP is increased, the lowest expected cost saving systematically occurs at a higher RR level.

References

[1] U.S. Department of Energy. 2015 Wind Technologies Market Report. [Online]. Available: http://energy.gov/sites/prod/files/2016/08/f33/2015-Wind-Technologies-Market-Report-08162016.pdf

[2] ——. 2015 Wind vision: A New Era for Wind Power in the United States. [Online]. Available: http://www.energy.gov/sites/prod/files/wv_executive_summary_overview_and_key_chapter_findings_final.pdf

[3] NREL. (2010) Western Wind and Solar Integration Study, National Renewable Energy Laboratrory, May.

[4] GE. (2010) New England Wind Integration Study Final Report, GE Energy Application and Systems Engineering, EnerNex Corporation and AWS Truepower.

[5] M. Milligan and et al., "Operational analysis and methods for wind integration studies," *IEEE Transactions on Sustainable Energy*, vol. 3, no. 4, pp. 612–619, 2012.

[6] EnerNex. (2014) NSP Wind Integration Study, August. [Online]. Available: https://www.xcelenergy.com/staticfiles/xe/PDF/Regulatory/16-App-M-NSP-Wind-Integration-Study-January-2015.pdf

[7] S. Abujarad, M. Mustafa, and J. Jamian, "Recent approaches of unit commitment in the presence of intermittent renewable energy resources: A review," *Renewable and Sustainable Energy Reviews*, vol. 70, pp. 215–223, 2017.

[8] D. Bertsimas, E. Litvinov, X. A. Sun, and et al., "Adaptive robust optimization for the security constrained unit commitment problem," *IEEE Transactions on Power Systems*, vol. 28, no. 1, pp. 52–63, 2013.

[9] Q. Wang, J. Wang, and Y. Guan, "Stochastic unit commitment with uncertain demand response," *IEEE Transactions on Power Systems*, vol. 28, no. 1, pp. 562–563, 2013.

[10] E. Ela. (2011) Impacts of Solar Power on Operating Reserve Requirements, august. [Online]. Available: http://www.nrel.gov/docs/fy13osti/56596.pdf

[11] Z. Zhou and A. Botterud, "Dynamic scheduling of operating reserves in co-optimized electricity markets with wind power," *IEEE Transactions on Power Systems*, vol. 29, no. 1, pp. 160–171, 2014.

[12] K. Hedman, M. Zhang, and M. Ilic, "Markets for ancillary services in the presence of stochastic resources," *PSERC Publication 16-06*, 2016.

[13] D. Krishnamurthy, W. Li, and L. Tesfatsion, "An 8-zone test system based on ISO New England data: Development and application," *IEEE Transactions on Power Systems*, vol. 31, no. 1, pp. 234–246, 2016. [Online]. Available: http://www2.econ.iastate.edu/tesfatsi/8ZoneISONETestSystem.RevisedAppendix.pdf

[14] AMES Wholesale Power Market Test Bed Homepage. [Online]. Available: http://www.econ.iastate.edu/tesfatsi/AMESMarketHome.htm

[15] FERC, "Notice of white paper," U.S. Federal Energy Regulatory Commission, April 2003.

[16] Y. Dvorkin, R. Fernández-Blanco, D. Kirschen, H. Pandžić, J. Watson, and C. Silva-Monroy, "Ensuring profitability of energy storage," *IEEE Transactions on Power Systems*, vol. 32, no. 1, pp. 611–623, 2017.

[17] B. Hua and R. Baldick. (2016) A convex primal formulation for convex hull pricing. [Online]. Available: https://arxiv.org/pdf/1605.05002v2.pdf

[18] B. Zhao, A. Conejo, and R. Sioshansi, "Unit commitment under gas-supply uncertainty and gas-price variability," *IEEE Transactions on Power Systems*, vol. 32, no. xx, pp. xx–xx, 2017.

[19] T. Xu, A. Birchfield, K. Genger, K. Shetye, and T. Overbye, "Application of large-scale synthetic power system models for energy economic studies," *Proceedings of the 50th Hawaii International Conference on System Sciences*, pp. 3123–3129, 2017.

[20] ISO-NE Homepage. [Online]. Available: http://www.iso-ne.com/

[21] D. Krishnamurthy. 8-Zone ISO-NE Test System: Code and Data Repository, created 2016. [Online]. Available: https://bitbucket.org/kdheepak/eightbustestbedrepo

[22] ISO NE. New England Wind Integration Study, 2013 Regional System Plan: Executive Summary. [Online]. Available: http://www.iso-ne.com/static-assets/documents/trans/rsp/2013/2013_rsp.pdf

[23] Wind Power Program. (2017) Wind Power Program Library: Wind Turbines, January. [Online]. Available: http://www.wind-power-program.com/library/turbine_leaflets/

[24] The Iowa Environmental Mesonet (IEM) Connecticut ASOS . [Online]. Available: https://mesonet.agron.iastate.edu/request/download.phtml?network=CT_ASOS

[25] The Iowa Environmental Mesonet (IEM) Homepage. [Online]. Available: https://mesonet.agron.iastate.edu/

[26] M. Carrion and J. Arroyo, "A computationally efficient mixed-integer linear formulation for the thermal unit commitment problem," *IEEE Trans. on Power Syst.*, vol. 21, no. 3, pp. 1371–1378, Aug 2006.

[27] ISO-NE Load Zone Data. [Online]. Available: https://www.iso-ne.com/isoexpress/web/reports/pricing/-/tree/zone-info

[28] H. Heitsch and W. Römisch, "Scenario reduction algorithms in stochastic programming," *Comp. Opt. Applic.*, vol. 24, no. 2-3, pp. 187–206, 2003.

[29] Y. Feng and S. M. Ryan, "Solution sensitivity-based scenario reduction for stochastic unit commitment," *Computational Management Science*, vol. 13, no. 1, pp. 29–62, 2016. [Online]. Available: http://dx.doi.org/10.1007/s10287-014-0220-z

Wanning Li (S'12) received the B.S. degree in electrical engineering from Harbin Institute of Technology, China, in 2011, and is completing a Ph.D. degree in the Department of Electrical and Computer Engineering at Iowa State University. She has been a research intern at MISO working on load forecasting, AGC enhancement with storage, and unit commitment process improvement. Currently she is a senior energy market specialist with the Integrated Planning Division of Southern California Edison, Rosemead, California. Her primary research areas are electric power market design and optimization of power system operations.

Leigh Tesfatsion (M'05) received the Ph.D. degree in economics from the U. of Minnesota, Mpls., in 1975. She is Professor of Economics, Mathematics, and Electrical and Computer Engineering at Iowa State University. Her principal research area is agent-based test bed development for coupled human and physical systems, with a special focus on electric power market design. She participates in various IEEE PES task forces focusing on power economics issues and serves as associate editor for a number of journals, including *J. of Energy Markets* and *J. of Economic Dynamics and Control*.